



Contents lists available at ScienceDirect

Bioorganic & Medicinal Chemistry

journal homepage: www.elsevier.com/locate/bmc

Design, synthesis, and functional assessment of Cmpd-15 derivatives as negative allosteric modulators for the β_2 -adrenergic receptor

Kaicheng Meng^{a,c}, Paul Shim^{b,c}, Qingtin Wang^a, Shuai Zhao^a, Ting Gu^a, Alem W. Kahsai^b, Seungkirl Ahn^b, Xin Chen^{a,*}

^aSchool of Pharmaceutical and Life Sciences, Changzhou University, Jiangsu 213164, China

^bDepartment of Medicine, Duke University Medical Center, Durham, NC 27710, USA

ARTICLE INFO

Article history:

Received 8 February 2018

Revised 12 March 2018

Accepted 14 March 2018

Available online xxxxx

Keywords:

 β_2 -Adrenergic receptor (β_2 AR)

Negative allosteric modulator

Synthesis

Structure-activity relationships

Binding competition assays

ABSTRACT

The β_2 -adrenergic receptor (β_2 AR), a G protein-coupled receptor, is an important therapeutic target. We recently described Cmpd-15, the first small molecule negative allosteric modulator (NAM) for the β_2 AR. Herein we report in details the design, synthesis and structure-activity relationships (SAR) of seven Cmpd-15 derivatives. Furthermore, we provide in a dose-response paradigm, the details of the effects of these derivatives in modulating agonist-induced β_2 AR activities (G-protein-mediated cAMP production and β -arrestin recruitment to the receptor) as well as the binding affinity of an orthosteric agonist in radio-ligand competition binding assay. Our results show that some modifications, including removal of the formamide group in the *para*-formamido phenylalanine region and bromine in the *meta*-bromobenzyl methylbenzamide region caused dramatic reduction in the functional activity of Cmpd-15. These SAR results provide valuable insights into the mechanism of action of the NAM Cmpd-15 as well as the basis for future development of more potent and selective modulators for the β_2 AR based on the chemical scaffold of Cmpd-15.

© 2018 Published by Elsevier Ltd.

1. Introduction

The β_2 -adrenergic receptor (β_2 AR) is a prototypical G protein-coupled receptor (GPCR) and is also an important therapeutic target for diseases such as cardiac arrhythmias, hypertension, and other cardiovascular diseases.^{1,2} Drugs that target the β_2 AR, such as β -blockers, are orthosteric β -adrenergic receptor antagonists that bind to the endogenous adrenaline binding site.^{3–6} To date, all known β -adrenergic agonists and antagonists are orthosteric ligands. However, the possibility that allosteric modulators that potentiate or attenuate the activity of orthosteric ligands might possess enhanced therapeutic efficacy, selectivity, or other novel therapeutic properties has raised interest in identifying and characterizing such modulators for the β_2 AR.

We recently carried out high throughput screening of DNA-encoded small-molecule libraries (DEL), comprising 190 million different unique compounds, against purified human β_2 AR. This *in vitro* affinity based screening approach yielded the first allosteric β -blocker, named as Cmpd-15⁷ (Scheme 1). The compound inhibits

agonist- β_2 AR induced G-protein activities (as measured via cAMP accumulation) and binds to inactive state form of the receptor with low micro-molar binding affinity. More recently, we co-crystallized and solved the structure of inactive β_2 AR in complex with Cmpd-15, in the form of a polyethylene glycol-carboxylic acid derivative (Cmpd-15PA). The structure reveals that the β_2 AR NAM Cmpd-15 ('allosteric β -blocker') binds to a pocket which is composed of the cytoplasmic ends of transmembrane segments 1, 2, 6 and 7 (TM1, TM2, TM6 and TM7) as well as intracellular loop 1 (ICL1) and helix 8 (H8). A proposed mechanism of allosteric antagonism of Cmpd-15 is that this modulator prevents β_2 AR from coupling to Gs, and blocks the interactions with arrestins.⁸ Herein we report in details the design and synthesis of seven Cmpd-15 derivatives, and present a more detailed dose dependent assessment for their ability to modulate agonist-mediated β_2 AR activities in downstream functional and radioligand binding competition assays.

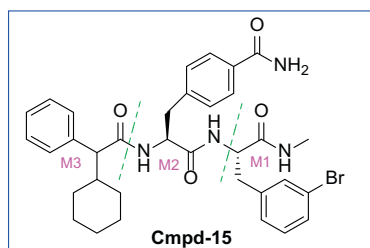
2. Design and synthesis of Cmpd-15 derivatives

The structure of Cmpd-15 is shown in Scheme 1. Guided by knowledge of the initial hits from our *in vitro* affinity-based selection with DEL described in our previous paper⁷, we designed 7 derivatives, focused on strategic points on the chemical structure

* Corresponding author.

E-mail address: xinchen@cczu.edu.cn (X. Chen).

^c These authors contributed equally to this work.



Scheme 1. Chemical structure of Cmpd-15.

of Cmpd-15; with the aim of investigating the influence of steric, hydrophilic, and hydrophobic features on NAM activity of the derivatives. For the convenience of our SAR analyses, the structure of Cmpd-15 is divided into three subunits (Scheme 1) similar to as previously described⁷: the (*meta*-bromobenzyl)methylbenzamide (M1), (*para*-formamido)phenyl-alanine (M2), and cyclohexyl-2-phenylacetamido (M3) regions. We made certain modifications in each region. For example, in region M1, an additional *meta*-bromine was introduced to the phenyl ring (derivative **15A5**), the *meta*-bromine was replaced with *meta*-fluorine (derivative **15A4**), and the *meta*-bromine was removed (**15A3**); in region M2, the *para*-formamide group was moved to the *meta*-position (**15A2**), and completely removed (**15A1**); in region M3, a methoxy group (**15A7**) and a hydroxyl group (**15A6**) were introduced to the *para*-position of the phenyl ring, respectively.

The synthetic route for the designed Cmpd-15 derivatives is outlined in Scheme 2. The chiral building block, substituted (*S*)-phenyl alanine **5a–5c**, was prepared through asymmetric phase transfer catalytic alkylation^{9–11} of substituted benzyl bromide with diphenylamine glycine *tert*-butyl ester **3**. The latter was obtained by condensation of benzophenone with glycine *tert*-butyl ester in refluxing toluene and in the presence of boron trifluoride diethyl etherate. Under the catalysis of *O*-allyl-*N*-9-anthracene methyl bromide cinchonine (**3A**), **3** was alkylated by substituted benzyl bromide in toluene/chloroform (2:1) and at $-40\text{ }^{\circ}\text{C}$, affording (*S*)-3-halobenzyl-2-diphenylimine glycine *tert*-butyl ester (**4a–4c**) in highly stereochemistry-controlled manner. For example, (*S*)-3-(3,5-dibromobenzyl)-2-diphenylimine glycine *tert*-butyl ester (**4a**) was obtained with 94.9% ee. After acidic hydrolysis in hydrochloric acid, **4a–4c** were converted into the corresponding *L*-phenyl alanines **5a–5c**, and then the amino group was protected with Fmoc, affording Fmoc-protected *L*-phenyl alanines **6a–6c**. The acidic hydrolysis didn't racemize the amino acids.¹² For example, the ee value of (9*H*-fluoren-9-yl)methyl (*S*)-(3,5-dibromo)-phenylalanine (**6a**) is 94.7%. In the next step, Fmoc-protected *L*-phenylalanine methylamides **7a–7d** were obtained by condensation of methylamine with the corresponding *L*-phenylalanines in the presence of *O*-benzotriazol-1-yl-*N,N,N',N'*-tetramethyluronium hexafluorophosphate (HBTU) and hydroxybenzotriazole (HOBT).¹³ Upon treatment with piperidine in DMF,¹³ the Fmoc group in **7a–7d** was removed smoothly, giving *L*-phenylalanine methylamides **8a–8d** with satisfactory yields.

With amines **8a–8d** in hand, we turn our attention to the remaining steps in the synthetic sequence. By employing HBTU/HOBT as the amide coupling agents, **8a–8d** were coupled with Fmoc-*L*-4-carbamoylphenylalanine (**9a**, $R_3 = 4$ -formamide), Fmoc-*L*-3-carbamoylphenylalanine (**9b**, $R_3 = 3$ -formamide) or Fmoc-*L*-phenylalanine (**9c**, $R_3 = \text{H}$), respectively, and dipeptides **10a–10f** were generated. Under the same reaction conditions used for preparation of **5a–5c**, the Fmoc group in **10a–10f** was taken off by piperidine and resulted in amines **11a–11f**. In the final step, **11a–11f** were reacted with 2-cyclohexyl-2-phenyl acetic acid (**14a**, $R_4 = \text{H}$), 2-cyclohexyl-2-(4-methoxyphenyl)acetic acid (**14b**,

$R_4 = 4\text{-OMe}$), and 2-cyclohexyl-2-(4-hydroxyphenyl)acetic acid (**14c**, $R_4 = 4\text{-OH}$), respectively, affording the desired final products (**15A1–15A7**). While **14a** is commercial available, **14b** was prepared by alkylation of 2-(4-methoxyphenyl)acetic acid with cyclohexyl 4-methylbenzenesulfonate in the presence of *n*-butyllithium (Scheme 3). Upon treatment with boron tribromide, **14b** was demethylated to give **14c** in 55% yield. The identity of all the products and the intermediates was confirmed by their ¹H NMR, ¹³C NMR and high-resolution mass spectrometry (HRMS) properties.

3. Pharmacological activity assays of Cmpd-15 derivatives

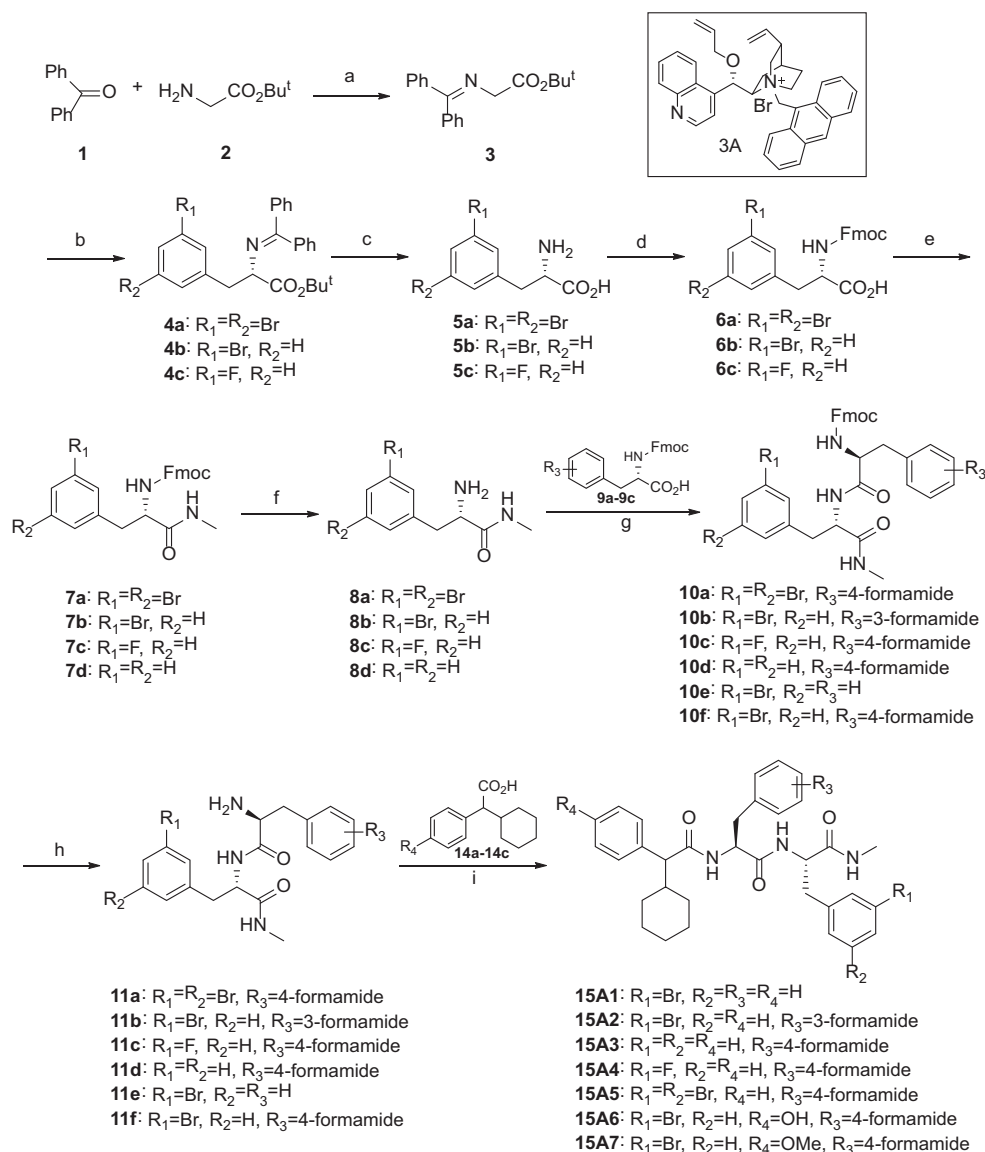
We conducted both cell-based assays and radioligand binding assays to characterize the pharmacological activity of seven derivatives of Cmpd-15 at the β_2 AR in a more systematic way than the previous report.⁷ The cell-based assays include the Promega GloSensor assay and the DiscoverX PathHunter assay. The Promega GloSensor assay was performed to measure agonist-induced cAMP production as a means of quantifying G-protein activation, and the DiscoverX PathHunter assay was performed to measure agonist-induced β -arrestin recruitment to the receptor. For the highly amplified GloSensor assay, HEK-293 cells endogenously expressing the β_2 AR were pretreated with the derivatives and then read after the stimulation with the orthosteric agonist, isoproterenol (ISO). For the stoichiometric DiscoverX PathHunter assay, U2OS cells stably expressing the chimeric β_2V_2R , which has increased phosphorylation on C-terminus tail, leading to more stable interaction with β -arrestin than the native receptor, were pretreated with the derivatives, and then stimulated with ISO. Competition binding with ¹²⁵I-cyanopindolol (CYP) was performed to determine the derivatives' ability to affect the binding of an orthosteric agonist to the β_2 AR. Both the allosteric derivatives and the orthosteric agonist isoproterenol (ISO) were introduced to reconstituted in High-Density-Lipoparticles (HDLs, or nanodiscs). The orthosteric antagonist ¹²⁵I-CYP was then introduced and allowed to compete with ISO in a dose-wise manner.

4. Results and discussion

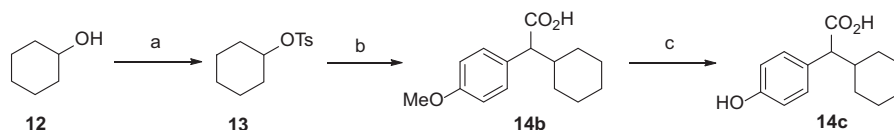
All the Cmpd-15 derivatives were systematically evaluated for their ability to modulate agonist-induced β_2 AR activities in a concentration-dependent manner by using two cellular functional assays (*G α s* signaling via cAMP accumulation measurement and β -arrestin recruitment) as well as a competition radio-ligand binding assay. The results are summarized in Tables 1 and 2.

Table 1 is the summary of the data showing the maximum degree of inhibition of E_{max} induced by a derivative relative to that of Cmpd-15. The data are consistent with the results in our previous report, in which we evaluated the inhibitory activity of these derivatives at a single concentration (50 μM).⁷ Table 2 shows the maximum fold shift of ISO IC_{50} or EC_{50} values induced by the derivatives at 50 μM in ¹²⁵I-CYP competition binding (IC_{50}) as well as both the GloSensor and PathHunter cell-based assays (EC_{50}).

The effect of Cmpd-15 and its derivatives **15A1–15A7** on β_2 AR-mediated functional activities is presented in Figs. 1–3. After pretreatment with Cmpd-15 or its derivatives at various concentrations, β_2 AR-mediated activity were measured in cells upon stimulation with isoproterenol (ISO) in a dose-dependent manner: cAMP production by the endogenously expressed β_2 AR (Fig. 1) and β -arrestin recruitment to the exogenously expressed β_2V_2R (Fig. 2). A dose-response curve of ISO competition binding to the β_2 AR reconstituted in HDL particles (nanodiscs) with radiolabeled ¹²⁵I-CYP and ISO was obtained in the presence of 50 μM of Cmpd-15 or its derivatives (Fig. 3). For Cmpd-15, there were both a decrease in E_{max} and a curve shift of the EC_{50} to the right in both the cAMP



Scheme 2. Synthetic route for Cmpd-15 derivatives **15A1–15A7**. Reagents and condition: (a) BF₃·Et₂O, toluene, reflux, 8 h; (b) **3A**, substituted benzyl bromide, 50% aq. KOH, toluene/CHCl₃, –40 °C, 72 h; (c) 6 N HCl, 100 °C, 3 h; (d) Fmoc-Cl, Na₂CO₃, dioxane, 0 °C–rt, 22 h; (e) MeNH₂·HCl, HBTU, HOBT, DIEA, DMF, rt, 12 h; (f) piperidine, DMF, rt, 2 h; (g) **9**, HBTU, HOBT, DIEA, DMF, rt; (h) piperidine, DMF, rt; (i) **14a–14c**, HBTU, HOBT, DIEA, DMF, rt.



Scheme 3. Synthetic routes for **14b** and **14c**. Reagents and condition: (a) TsCl, pyridine, rt, 12 h, 79%; (b) 2-(4-methoxyphenyl)acetic acid, *n*-BuLi, –78 °C–25 °C, 13 h, 43%; (c) BBr₃, DCM, 0 °C–25 °C, 40 h, 55%.

production and β -arrestin recruitment to the active receptor (Figs. 1A and 2A). There was a right curve shift in the ¹²⁵I-CYP competition-binding assay (Fig. 3A). Overall, we recapitulated the inhibitory activity of Cmpd-15 with the similar extent to what we obtained in our previous report.⁷

For derivative **15A5** which contains a second *meta*-bromine group in the region M1, there was both a decrease in E_{max} and a curve shift of the EC₅₀ to the right in both the cAMP production and β -arrestin recruitment assays (Figs. 1F and 2F), although to a lesser degree compared to Cmpd-15. We observed a greater degree

of inhibition mediated by **15A5** in β -arrestin recruitment than in cAMP production. There was a right curve shift in the ¹²⁵I-CYP competition-binding assay (Fig. 3F). It is possible that this second bromine group may reduce **15A5** functional activity by decreasing the affinity of the compound to its binding pocket due to increased steric effects.

When the bromine was replaced with fluorine in the region M1 (**15A4**), there was no significant inhibition of E_{max} or a curve shift of the EC₅₀ in both the cAMP production and β -arrestin recruitment assays (Figs. 1E and 2E). There was a small curve shift of the IC₅₀ to

Table 1
Comparison of the allosteric modulation activity of **15A1–15A7** to Cmpd-15.

Compound (50 μ M)	Inhibitory Activity (%) ^a	
	Cell-based activity	
	cAMP	β -Arr
Cmpd-15	100	100
15A1	11 \pm 10	21 \pm 4
15A2	46 \pm 10	50 \pm 4
15A3	12 \pm 11	15 \pm 2
15A4	10 \pm 8	23 \pm 5
15A5	38 \pm 6	65 \pm 4
15A6	-2 \pm 5	7 \pm 4
15A7	13 \pm 5	47 \pm 6

^a Values are expressed as percentages of the Cmpd-15 blockade level in each assay and represent mean \pm SEM obtained from at least three independent experiments. Statistical analysis was performed as described in 6.4 Data Analysis of Experimental Section. All of the values obtained with analogs are significantly different ($P < 0.001$) compared to the inhibition obtained by Cmpd-15, which was normalized to 100%.

Table 2
Comparison of the EC₅₀ fold shift for derivatives **15A1–15A7** in the ¹²⁵I-CYP competition binding and cell-based assays.

Compound (50 μ M)	IC ₅₀ or EC ₅₀ Fold Shift ^a		
	¹²⁵ I-CYP competition binding	Cell-based activity	
		cAMP	β -Arr
Cmpd-15	5.4 \pm 0.68	3.6 \pm 0.62	7.0 \pm 1.32
15A1	0.9 \pm 0.03***	0.7 \pm 0.09***	1.5 \pm 0.14***
15A2	1.3 \pm 0.06***	1.4 \pm 0.27**	1.4 \pm 0.29**
15A3	1.1 \pm 0.30***	1.1 \pm 0.28**	1.3 \pm 0.07***
15A4	2.1 \pm 0.06***	0.9 \pm 0.12***	0.8 \pm 0.09***
15A5	4.6 \pm 0.37	2.3 \pm 0.10	2.6 \pm 0.28**
15A6	1.2 \pm 0.44***	1.2 \pm 0.22**	1.1 \pm 0.09***
15A7	0.8 \pm 0.07***	1.2 \pm 0.18***	1.1 \pm 0.25***

^a Values are expressed as the fold-shift of either the EC₅₀ value (cell-based assays) or the IC₅₀ value (competition binding assay) of the ISO curve in the presence of each derivative compared to that obtained DMSO-treated control curve. They represent mean \pm SEM obtained from at least three independent experiments. Statistical analysis was performed as described in 6.4 Data Analysis of Experimental Section. ** $P < 0.01$; *** $P < 0.001$ compared to the fold shift of the EC₅₀ obtained by Cmpd-15.

the right in the ¹²⁵I-CYP competition-binding assay (Fig. 3E). It appears to be the smaller size of the fluorine group which causes the lack of allosteric activity of the analog since bromine and fluorine are comparable in electronegativity.

After the bromine group was removed from the phenyl ring in the region M1, the resulting derivative **15A3** has no significant inhibition of E_{max} or a curve shift of the EC₅₀ in both of the cell-based functional assays (Figs. 1D and 2D). Also, there was no curve shift of the IC₅₀ in the ¹²⁵I-CYP competition-binding assay (Fig. 3D). This data shows that the bromine group has a critical role in Cmpd-15's functional activity, also supported by the previous X-ray crystallographic study.⁸

In the region M2, when the formamide group is in the *meta*-position compared to the *para*-position of Cmpd-15 (**15A2**), there was both a decrease in E_{max} and a curve shift of the EC₅₀ to the right in both the cAMP production and β -arrestin recruitment assays, although to a lesser degree compared to Cmpd-15 (Figs. 1C and 2C). There was no curve shift of the IC₅₀ in the ¹²⁵I-CYP competition-binding assay (Fig. 3C). It is possible that this *meta*-position of the formamide reduces **15A2**'s functional activity by

robustly decreasing the affinity of the compound to its binding pocket due to increased steric effects.

After the formamide group was removed from the phenyl ring in the region M2, there was no significant inhibition of E_{max} or a curve shift of the EC₅₀ for the resulting derivative **15A1** in both of the cell-based functional assays (Figs. 1B and 2B). There was also no curve shift of the IC₅₀ in the ¹²⁵I-CYP competition-binding assay with **15A1** (Fig. 3B). These results indicate that the formamide group also has a critical role in Cmpd-15's functional activity, as supported by the previous X-ray crystallographic study.⁸

In the region M3, when a hydroxy group was introduced to the *para*-position of the phenyl group, there was no significant inhibition of E_{max} or a curve shift of the EC₅₀ for the resulting derivative **15A6** in either the Glosensor and the PathHunter assays, and there was no curve shift of the IC₅₀ in the ¹²⁵I-CYP competition-binding assay (Figs. 1G–3G). This suggests that the hydrophobic nature of the M3 region is important for Cmpd-15's functional activity as suggested by our previous X-ray crystallographic study.⁸

For derivative **15A7** which contains a *para*-methoxy group in the region M3, there was no significant inhibition of E_{max} or a curve shift of the EC₅₀ in the cAMP production assay (Fig. 1H) while there was both a small decrease in E_{max} and a curve shift of the EC₅₀ to the right in the β -arrestin recruitment assays (Fig. 2H). We also observed no curve shift of the IC₅₀ in the ¹²⁵I-CYP competition-binding assay with **15A7** (Fig. 3H). The presence of β -arrestin recruitment inhibition strongly supports the claim that the hydrophobic nature of the region M3 is important for Cmpd-15's functional activity, as a methoxy group is less hydrophilic than a hydroxyl group.

Our SAR analysis here in this study is also consistent with molecular interactions observed between Cmpd-15 and the residues of the binding site in the recently solved co-crystal structure of β_2 AR–Cmpd-15 PA (Fig. 4). According to the co-crystal structure of Cmpd-15PA with β_2 AR,⁸ the *meta*-bromobenzyl ring in region M1 of Cmpd-15PA forms a cation- π interaction with Arg63^{ICL1} in ICL1 of the β_2 AR; the *para*-formamido group in region M2 of Cmpd-15PA forms polar interactions with side chains of Thr274^{6.36} in TM6 and Arg328^{7.55} in TM7 of the β_2 AR. For region M3, the cyclohexyl and phenyl rings form hydrophobic interactions with the hydrophobic residues from β_2 AR, composing of Val54^{1.53} and Ile58^{1.57} at the end of TM1, Leu64^{ICL1} in ICL1, Ile72^{2.43} in TM2, Leu275^{6.37} in TM6, Tyr326^{7.53} in TM7, and Phe332^{8.50} in H8.⁸

5. Conclusion

We have designed and synthesized seven derivatives of Cmpd-15 and carried out a structure-activity relationship study to examine their effects on agonist-induced β_2 AR activities. The pharmacological profiles of these analogs were evaluated for their effects at agonist-mediated G α s signaling (via cAMP accumulation measurement) and β -arrestins recruitment to active receptor as well as competitive radio-ligand agonist binding experiments, all with a dose-response paradigm. The present study demonstrates that Cmpd-15 derivatives with formamide group in the region M2 as well as bromine group in the region M1 are critical in its ability for modulating the agonist-induced activity of β_2 AR. These were observed by the fact that complete deletions of the two groups dramatically decreased the agonist-induced β_2 AR G-protein activity and recruitment of β -arrestin compared to the parent compound. It was also found that the increased polarity in region M3 is closely associated with the loss of functional effects of Cmpd-15 at the agonist induced β_2 AR activities. Hence, this further ascertains the M3 region of Cmpd-15's interaction with the core hydrophobic residues within the β_2 AR allosteric site, consistent with the pro-

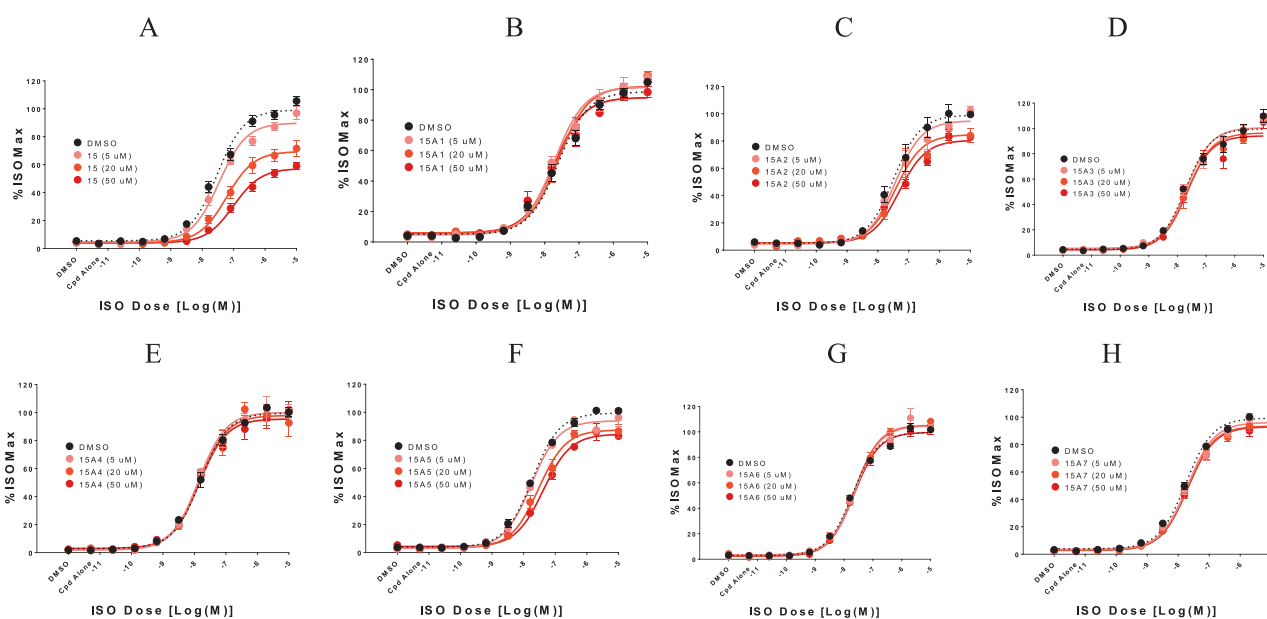


Fig. 1. Pharmacological activity of Cmpd-15 and its derivatives **15A1–15A7**: cAMP production by the endogenously expressed β_2 AR. (A) Cmpd-15, (B) **15A1**, (C) **15A2**, (D) **15A3**, (E) **15A4**, (F) **15A5**, (G) **15A6**, (H) **15A7**. Values were expressed as percentages of the maximal level of the isoproterenol-induced activity in the vehicle (DMSO) control. Points on curves represent mean \pm SEM obtained from at least three independent experiments done in duplicate.

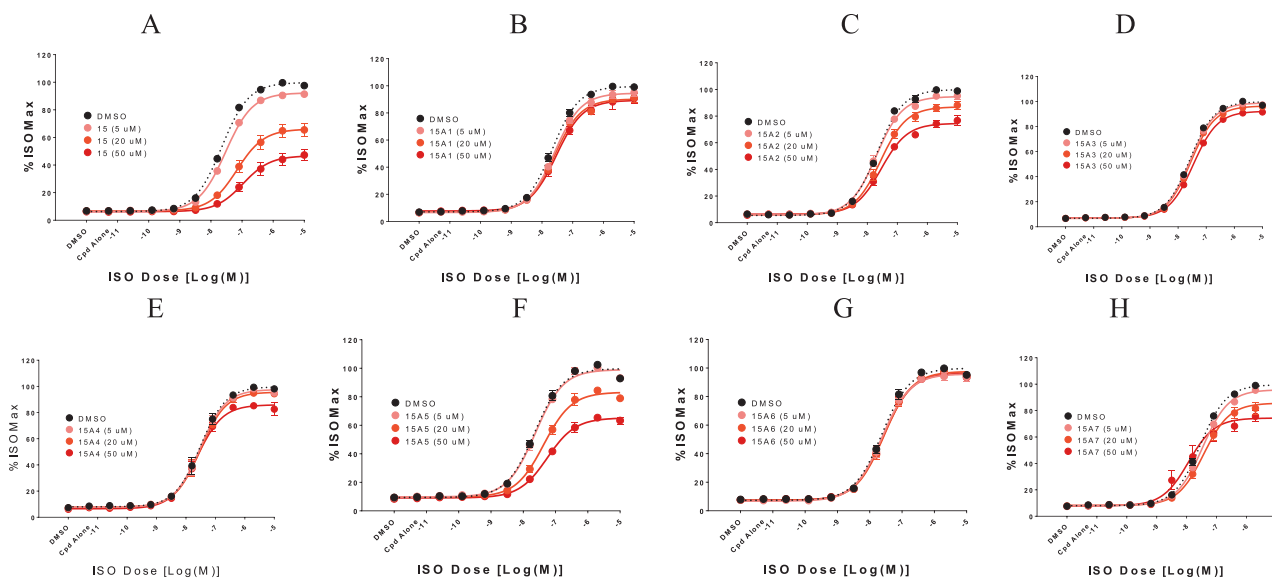


Fig. 2. Pharmacological activity assays for Cmpd-15 and its derivatives **15A1–15A7**: β -arrestin recruitment to the stably over-expressed β_2 V₂R. (A) Cmpd-15, (B) **15A1**, (C) **15A2**, (D) **15A3**, (E) **15A4**, (F) **15A5**, (G) **15A6**, (H) **15A7**. Values were expressed as percentages of the maximal level of the isoproterenol-induced activity in the vehicle (DMSO) control. Points on curves represent mean \pm SEM obtained from at least three independent experiments done in duplicate.

posed modes of binding of the compound in the recently solved X-ray crystal structure of Cmpd-15 in complex with β_2 AR. Together, the identification of the Cmpd-15 type chemical preferences and detailed characterization of the novel Cmpd-15 binding allosteric site at the β_2 AR should provide insight into designing and developing specific therapies in blocking β -receptor activities.

6. Experimental Section

6.1. Chemistry

All chemical reagents were purchased from Energy Chemicals and Aladdin Chemicals (Shanghai, China) and used as received.

All moisture-sensitive reactions were carried out using anhydrous solvents and under nitrogen atmosphere. ^1H and ^{13}C NMR spectra were recorded on a Bruker Avance III spectrometer (300 MHz and 400 MHz) using TMS as the internal standard. High resolution mass spectrometry (HRMS) was performed on Agilent Technologies 6540 UHD Accurate-Mass Q-TOF. Flash column chromatography was performed with silica gel (300–400 mesh).

6.1.1. (9H-Fluoren-9-yl)methyl (S)-(3,5-dibromo)phenylalanine (**6a**)

To a solution of benzophenone (3g, 16.4 mmol) and glycine *tert*-butyl ester (1.8 g, 13.7 mmol) in anhydrous toluene (18 mL) was added boron trifluoride diethyl etherate (0.12 mL), and the mixture was refluxed at 130 °C for 8 h. After removal of the solvent *in*

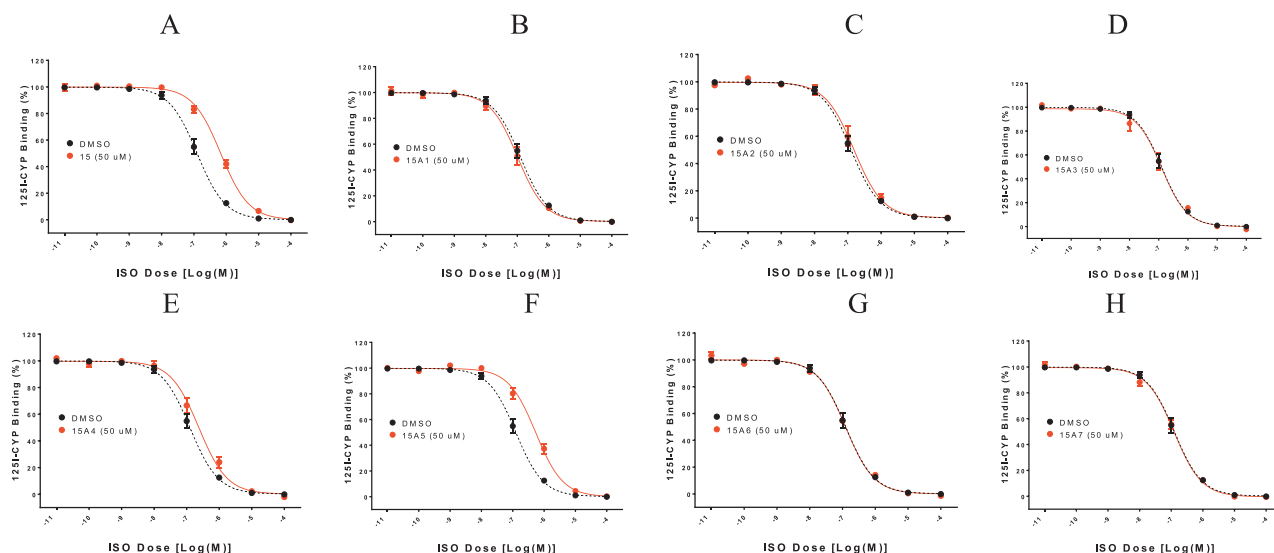


Fig. 3. Pharmacological activity assays for Cmpd-15 and its derivatives **15A1–15A7**: ISO competition binding to the β_2 AR reconstituted in nanodiscs with ^{125}I -CYP. (A) Cmpd-15, (B) **15A1**, (C) **15A2**, (D) **15A3**, (E) **15A4**, (F) **15A5**, (G) **15A6**, (H) **15A7**. Values were expressed as percentages of the maximal level of ^{125}I -CYP binding in the vehicle (DMSO) control. Points on curves represent mean \pm SEM obtained from at least three independent experiments done in duplicate.

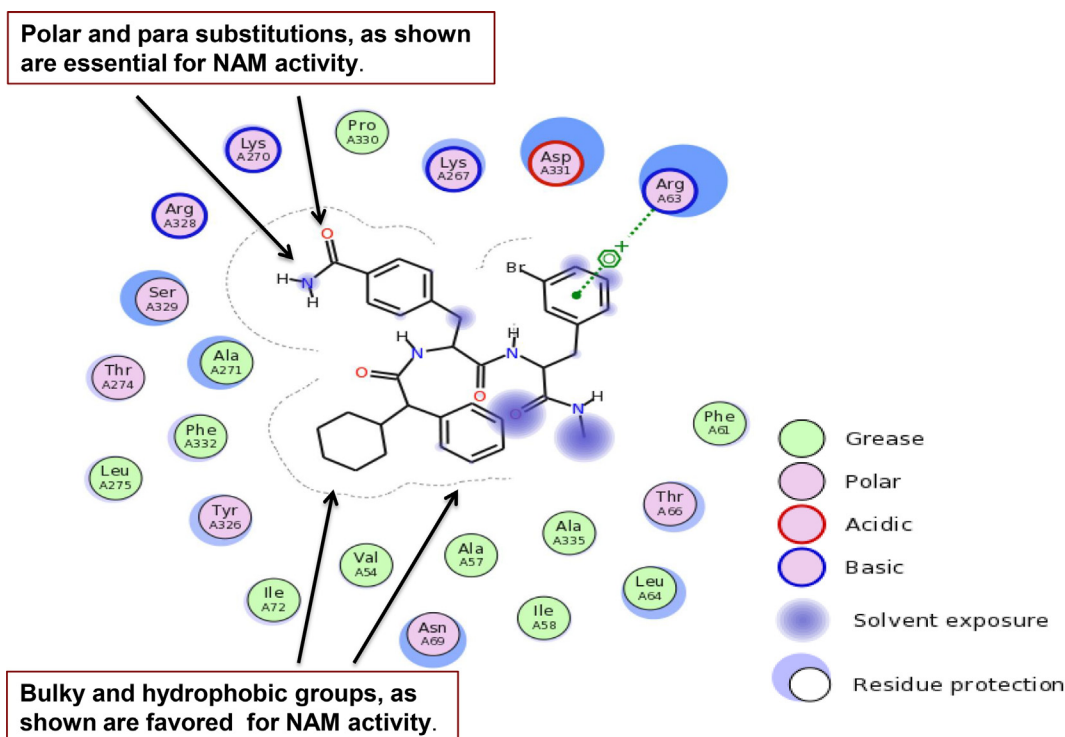


Fig. 4. 2D projection of the interactions of Cmpd-15 with the allosteric binding site at the β_2 AR. Schematic representations of the favored interactions (polar and nonpolar) of Cmpd-15 on the β_2 AR (PDB: 5X7D).

vacuo, the residue was dissolved in EtOAc (100 mL), and washed with H_2O (2×30 mL) and brine (2×30 mL), and dried (anhydrous Na_2SO_4). The crude product was purified by flash column chromatography (eluting with hexane/EtOAc, 20:1) to afford *N*-(diphenylamino)glycine *tert*-butyl ester (**3**) (1.4 g, 40% yield) as white solid. M.p. 112–113 °C; ^1H NMR (300 MHz, CDCl_3): δ 1.46 (s, 9H), 4.12 (s, 2H), 7.17–7.20 (m, 2H), 7.30–7.48 (m, 6H), 7.65–7.68 (m, 2H); ^{13}C NMR (75 MHz, CDCl_3): δ 28.2, 56.4, 81.2, 128.1, 128.9, 130.5, 139.5, 170.0, 171.6; HRMS (ESI, positive): Calcd. for $\text{C}_{19}\text{H}_{21}\text{NO}_2\text{Na}$ [$\text{M}+\text{Na}$] $^+$ 318.1465; observed: 318.1463.

50% KOH aqueous solution (0.44 mL, 7.8 mmol) was added to a stirred solution of **3** (458 mg, 1.55 mmol), 3,5-dibromobenzyl bromide (2.55 g, 7.76 mmol, 5 equiv) and *O*-allyl-*N*-9-anthracene methyl bromide cinchonine (**3A**) (94 mg, 0.15 mmol) in toluene/chloroform (22 mL, 2:1 v/v) at -40 °C, and the whole mixture was stirred at the same temperature for 72 h. After being warmed to ambient temperature, the reaction mixture was diluted with H_2O (100 mL), and the resulting mixture was extracted with EtOAc (3×80 mL). The combined EtOAc extracts were washed with brine (2×50 mL), and dried (anhydrous Na_2SO_4). The crude product was

purified by flash column chromatography (eluting with hexane/EtOAc, 20:1) to give (*S*)-3-(3,5-dibromobenzyl)-2-diphenylimine glycine *tert*-butyl ester (**4a**) as light yellow oil (0.7 g, 83% yield). $[\alpha]_D^{20} - 89.9$ ($c = 1.38$, CH_2Cl_2), 94.9% ee; $^1\text{H NMR}$ (300 MHz, CDCl_3): δ 1.37 (s, 9H), 3.01–3.15 (m, 2H), 4.05 (q, $J = 4.5$ Hz, 1H), 6.51–6.57 (m, 3H), 6.70 (d, $J = 6.0$ Hz, 2H), 7.19–7.26 (m, 6H), 7.27–7.33 (m, 2H); $^{13}\text{C NMR}$ (75 MHz, CDCl_3): δ 28.2, 39.8, 65.3, 81.4, 125.4, 128.4, 128.9, 130.3, 132.7, 132.9, 137.7, 139.6, 170.8, 170.9; HRMS (ESI, positive): Calcd. for $\text{C}_{26}\text{H}_{25}\text{Br}_2\text{NO}_2$ $[\text{M}+\text{H}]^+$ 542.0252, 544.0236; observed: 542.0326, 544.0310.

A mixture of **4a** (132 mg, 0.36 mmol) and 6 M HCl (5 mL) was heated at 100 °C for 3 h, and then the solvent and volatiles were removed by a rotary evaporator to give (*S*)-3,5-dibromo phenylalanine hydrochloride (**5a**) (100 mg, 78% yield) as white solid. The product was used for the next step without further purification. M.p. 245–246 °C; $^1\text{H NMR}$ (300 MHz, $\text{DMSO}-d_6$): δ 3.16 (q, $J = 4.5$ Hz, 2H), 4.18 (t, $J = 4.5$ Hz, 1H), 7.56 (s, 2H), 7.74 (s, 1H); $^{13}\text{C NMR}$ (75 MHz, $\text{DMSO}-d_6$): δ 34.6, 52.7, 122.5, 131.8, 132.2, 140.1, 170.0; HRMS (ESI, positive): Calcd. for $\text{C}_9\text{H}_9\text{Br}_2\text{NO}_2$ $[\text{M}+\text{H}]^+$ 321.9000, 323.8980; observed: 321.9073, 323.9053.

To an ice-cold solution of **5a** (135 mg, 0.37 mmol), dioxane (0.5 mL) and 10% Na_2CO_3 aqueous solution (1 mL) was added dropwise a solution of Fmoc-Cl (97 mg, 0.37 mmol) in dioxane (1 mL). The mixture was stirred at 0 °C for 4 h, and then warmed to ambient temperature with the stirring continued for additional 18 h. The reaction was quenched by adding 2 M HCl (2 mL) and H_2O (40 mL). The resulting mixture was extracted with EtOAc (2×60 mL), and the combined extracts were washed with brine (2×30 mL), and dried. The crude product was purified by flash column chromatography (eluting with hexane/EtOAc, 20:1) to give (9*H*-fluoren-9-yl)methyl (*S*)-(3,5-dibromo)phenylalanine (**6a**) (105 mg, 51% yield) as white solid. M.p. 238–239 °C; 94.7% ee. $^1\text{H NMR}$ (400 MHz, $\text{DMSO}-d_6$): δ 2.84 (q, $J = 10.8$ Hz, 1H), 3.10 (dd, $J = 13.7$, 3.8 Hz, 1H), 4.15–4.22 (m, 4H), 7.29 (q, $J = 8.0$ Hz, 2H), 7.40 (t, $J = 7.2$ Hz, 2H), 7.53 (d, $J = 1.2$ Hz, 2H), 7.60–7.63 (m, 2H), 7.68 (s, 1H), 7.76 (d, $J = 6.3$ Hz, 1H), 7.86 (d, $J = 5.7$ Hz, 2H); $^{13}\text{C NMR}$ ($\text{DMSO}-d_6$, 100 MHz): δ 35.6, 46.6, 55.0, 65.8, 120.1, 122.1, 125.2, 125.3, 127.1, 127.7, 131.5, 140.7, 143.0, 143.8, 156.0, 172.9; HRMS (ESI, negative): Calcd. for $\text{C}_{24}\text{H}_{19}\text{Br}_2\text{NO}_4$ $[\text{M}-\text{H}]^-$ 541.9608, 543.9588; observed: 541.9600, 543.9581.

6.1.2. (9*H*-Fluoren-9-yl)methyl (*S*)-(3-bromo)phenylalanine (**6b**)

By following the procedure used for preparing **6a**, (9*H*-fluoren-9-yl)methyl (*S*)-(3-bromo)phenylalanine (**6b**) was obtained by replacing 3,5-dibromobenzyl bromide with 3-bromobenzyl bromide. $^1\text{H NMR}$ (300 MHz, $\text{DMSO}-d_6$): δ 2.82–2.90 (m, 1H), 3.09 (dd, $J = 13.8$, 4.2 Hz, 1H), 4.14–4.22 (m, 4H), 7.21–7.34 (m, 4H), 7.41 (dd, $J = 7.5$, 1.2 Hz, 3H), 7.52 (s, 1H), 7.61 (t, $J = 6.6$ Hz, 2H), 7.80 (d, $J = 8.4$ Hz, 3H); $^{13}\text{C NMR}$ (75 MHz, $\text{DMSO}-d_6$): δ 36.6, 46.7, 56.0, 65.7, 120.2, 125.3, 127.2, 127.8, 128.1, 129.3, 130.0, 132.8, 140.8, 141.3, 143.0, 143.9, 156.0, 172.9; HRMS (ESI, positive): Calcd. for $\text{C}_{24}\text{H}_{20}\text{BrNO}_4\text{Na}$ $[\text{M}+\text{Na}]^+$ 488.0468, 490.0447; observed: 488.0466, 490.0447.

6.1.3. (9*H*-Fluoren-9-yl)methyl (*S*)-(3-fluoro)phenylalanine (**6c**)

By following the procedure used for preparing **6a**, (9*H*-fluoren-9-yl)methyl (*S*)-(3-fluoro)phenylalanine (**6c**) was obtained by replacing 3,5-dibromobenzyl bromide with 3-fluorobenzyl bromide. M.p. 145–148 °C; $^1\text{H NMR}$ (300 MHz, $\text{DMSO}-d_6$): δ 2.88–2.96 (m, 1H), 3.15 (dd, $J = 17.9$, 6.4 Hz, 1H), 4.15–4.29 (m, 4H), 7.01–7.18 (m, 3H), 7.26–7.42 (m, 8H), 7.62 (dd, $J = 9.6$, 5.6 Hz, 3H); $^{13}\text{C NMR}$ (75 MHz, $\text{DMSO}-d_6$): δ 36.6, 47.0, 55.7, 66.1, 113.8, 116.6, 120.6, 125.5, 125.7, 127.5, 128.1, 130.4, 141.1, 141.3, 144.2, 156.4, 173.7; HRMS (ESI, negative): Calcd. for $\text{C}_{24}\text{H}_{20}\text{FNO}_4$ $[\text{M}-\text{H}]^-$ 404.1304; observed: 404.1300.

6.1.4. General procedure for preparation of compounds **7a–7d**

Methylamine hydrochloride (87 mg, 1.3 mmol) and *N,N*-diisopropylethylamine (DIEA, 250 mg, 2 mmol) was added successively to an ice-cold stirred solution of the substituted (*S*)-phenylalanine **6a–6c** (0.64 mmol), HOBt (174 mg, 1.3 mmol) and HBTU (488 mg, 1.3 mmol) in DMF (6 mL) at 0 °C. The reaction mixture was stirred for 30 min at the same temperature, and then allowed to warm to ambient temperature while the stirring was continued for additional 12 h. The solvents and volatiles were removed under the reduced pressure, and the residue was dissolved in EtOAc (100 mL), and then washed with saturated NaHCO_3 solution (30 mL) and brine (2×30 mL), respectively, and dried (anhydrous Na_2SO_4). After the solvent was concentrated, the crude product was crystallized from EtOAc to give the desired product as white fluffy solid.

6.1.4.1. (9*H*-Fluoren-9-yl)methyl (*S*)-(3-(3,5-dibromophenyl)-1-(methylamino)-1-oxopropan-2-yl)carbamate (**7a**). 56% yield; $^1\text{H NMR}$ (400 MHz, $\text{DMSO}-d_6$): δ 2.59 (d, $J = 6.0$ Hz, 3H), 2.71–2.76 (m, 1H), 2.95 (dd, $J = 18.2$, 5.2 Hz, 1H), 4.09–4.21 (m, 4H), 7.26–7.43 (m, 4H), 7.56–7.87 (m, 6H), 7.87 (d, $J = 10.0$ Hz, 2H), 8.01 (d, $J = 6.0$ Hz, 1H); $^{13}\text{C NMR}$ (100 MHz, $\text{DMSO}-d_6$): δ 26.0, 37.2, 47.0, 56.5, 66.2, 120.6, 122.5, 125.8, 127.5, 128.1, 131.8, 141.0, 141.1, 143.8, 144.2, 156.3, 171.9; HRMS (ESI, positive): Calcd. for $\text{C}_{25}\text{H}_{22}\text{Br}_2\text{N}_2\text{O}_3\text{Na}$ $[\text{M}+\text{Na}]^+$ 578.9889, 580.9869; observed: 578.9886, 580.9869.

6.1.4.2. (9*H*-Fluoren-9-yl)methyl (*S*)-(3-(3-bromophenyl)-1-(methylamino)-1-oxopropan-2-yl)carbamate (**7b**). 94% yield; $^1\text{H NMR}$ (300 MHz, $\text{DMSO}-d_6$): δ 2.56 (d, $J = 4.8$ Hz, 3H), 2.79–2.98 (m, 4H), 3.16 (s, 1H), 4.45 (d, $J = 6.8$ Hz, 1H), 7.14–7.44 (m, 7H), 7.75 (d, $J = 8.4$ Hz, 2H), 7.90 (d, $J = 4.2$ Hz, 2H), 8.11 (d, $J = 7.8$ Hz, 1H); $^{13}\text{C NMR}$ (75 MHz, $\text{DMSO}-d_6$): δ 25.6, 37.2, 46.6, 56.2, 65.7, 120.1, 121.4, 125.4, 126.3, 127.7, 128.0, 129.1, 129.9, 132.7, 140.7, 141.0, 143.9, 155.9, 171.6; HRMS (ESI, positive): Calcd. for $\text{C}_{25}\text{H}_{23}\text{BrN}_2\text{O}_3$ $[\text{M}+\text{H}]^+$ 501.0784, 503.0764; observed: 501.0779, 503.0763.

6.1.4.3. (9*H*-Fluoren-9-yl)methyl (*S*)-(3-(3-fluorophenyl)-1-(methylamino)-1-oxopropan-2-yl)carbamate (**7c**). 64% yield; $^1\text{H NMR}$ (300 MHz, $\text{DMSO}-d_6$): δ 2.60 (d, $J = 6.0$ Hz, 3H), 2.79 (t, $J = 14.0$ Hz, 1H), 2.98 (dd, $J = 13.5$, 5.6 Hz, 1H), 4.12–4.19 (m, 4H), 7.02 (t, $J = 9.0$ Hz, 1H), 7.12–7.43 (m, 7H), 7.63 (t, $J = 6.0$ Hz, 2H), 7.71 (d, $J = 8.1$ Hz, 1H), 7.86–7.99 (m, 3H); $^{13}\text{C NMR}$ (75 MHz, $\text{DMSO}-d_6$): δ 25.7, 37.3, 46.7, 56.2, 65.8, 113.3, 115.9, 116.2, 120.2, 125.5, 127.2, 127.8, 130.1, 140.8, 141.4, 143.8, 143.9, 155.9, 171.7; HRMS (ESI, positive): Calcd. for $\text{C}_{25}\text{H}_{23}\text{FN}_2\text{O}_3\text{Na}$ $[\text{M}+\text{Na}]^+$ 441.1585; observed: 441.1580.

6.1.4.4. (9*H*-Fluoren-9-yl)methyl (*S*)-(1-(methylamino)-1-oxo-3-phenylpropan-2-yl)carbamate (**7d**). 88% yield; $^1\text{H NMR}$ (300 MHz, $\text{DMSO}-d_6$): δ 2.58 (d, $J = 6.0$ Hz, 3H), 2.78 (dd, $J = 18.0$, 8.4 Hz, 1H), 2.93–2.99 (m, 1H), 4.10–4.18 (m, 4H), 7.17–7.44 (m, 10H), 7.62–7.67 (m, 3H), 7.87 (d, $J = 9.6$ Hz, 2H), 7.95 (s, 1H); $^{13}\text{C NMR}$ (75 MHz, $\text{DMSO}-d_6$): δ 26.0, 37.7, 47.0, 56.5, 66.1, 113.4, 116.5, 120.6, 125.8, 127.5, 128.1, 130.3, 130.4, 141.1, 141.8, 156.3, 172.1; HRMS (ESI, positive): Calcd. for $\text{C}_{25}\text{H}_{24}\text{N}_2\text{O}_3\text{Na}$ $[\text{M}+\text{Na}]^+$ 423.1679; observed: 423.1679.

6.1.5. General procedure for preparation of compounds **8a–8d**

To a stirred solution of **7a–7d** (0.21 mmol) in DMF (4 mL) was added piperidine (2 mL) at room temperature. The reaction mixture was stirred at ambient temperature and under nitrogen atmosphere for 2 h. The solvent and volatiles were removed under reduced pressure, and the residue was purified by flash column chromatography (eluting with DCM/MeOH, 20:1) to afford (*S*)-2-amino-3-aryl-*N*-methylpropanamides (**8a–8d**) as light yellow solid.

6.1.5.1. (*S*)-2-Amino-3-(3,5-dibromophenyl)-*N*-methylpropanamide (**8a**). 90% yield; ^1H NMR (300 MHz, DMSO- d_6): δ 2.49 (d, J = 1.8 Hz, 3H), 2.51–2.63 (m, 1H), 2.85 (dd, J = 13.8, 6.0 Hz, 1H), 3.31 (dd, J = 8.4, 5.1 Hz, 1H), 7.18–7.26 (m, 2H), 7.36–7.41 (m, 1H), 7.81 (d, J = 4.5 Hz, 1H); ^{13}C NMR (75 MHz, DMSO- d_6): δ 25.8, 40.5, 56.4, 122.4, 131.4, 131.8, 144.5, 174.8; HRMS (ESI, positive): Calcd. for $\text{C}_{10}\text{H}_{12}\text{Br}_2\text{N}_2\text{O}_5\text{Na}$ $[\text{M}+\text{Na}]^+$ 356.9209, 358.9188; observed: 356.9208, 358.9192.

6.1.5.2. (*S*)-2-Amino-3-(3-bromophenyl)-*N*-methylpropanamide (**8b**). 75% yield; ^1H NMR (300 MHz, DMSO- d_6): δ 2.49 (d, J = 4.8 Hz, 3H), 2.51–2.63 (m, 1H), 2.88 (dd, J = 18.6, 6.8 Hz, 1H), 3.31 (dd, J = 11.2, 6.4 Hz, 1H), 7.18–7.26 (m, 2H), 7.36–7.41 (m, 1H), 7.81 (d, J = 6.0 Hz, 1H); ^{13}C NMR (75 MHz, DMSO- d_6): δ 25.5, 40.2, 56.3, 121.5, 128.5, 129.0, 130.2, 132.1, 142.1, 174.7; HRMS (ESI, positive): Calcd. for $\text{C}_{10}\text{H}_{13}\text{BrN}_2\text{O}_5\text{Na}$ $[\text{M}+\text{Na}]^+$ 257.0284, 259.0264; observed: 257.0285, 259.0265.

6.1.5.3. (*S*)-2-Amino-3-(3-fluorophenyl)-*N*-methylpropanamide (**8c**). 91% yield; ^1H NMR (400 MHz, DMSO- d_6): δ 2.53 (d, J = 2.0 Hz, 2H), 2.58–2.68 (m, 1H), 2.93 (dd, J = 17.6, 6.4 Hz, 1H), 6.99–7.04 (m, 3H), 7.27 (dd, J = 10.4, 9.6 Hz, 1H), 7.86 (d, J = 4.4 Hz, 1H); ^{13}C NMR (100 MHz, DMSO- d_6): δ 25.4, 40.1, 56.3, 121.4, 128.5, 128.9, 130.2, 132.0, 142.0, 174.7; HRMS (ESI, positive): Calcd. for $\text{C}_{10}\text{H}_{13}\text{FN}_2\text{O}_5\text{Na}$ $[\text{M}+\text{H}]^+$ 197.1085; observed: 197.1090.

6.1.5.4. (*S*)-2-Amino-*N*-methyl-3-phenylpropanamide (**8d**). 70% yield; m.p. 58–60 °C; ^1H NMR (300 MHz, DMSO- d_6): δ 2.66 (d, J = 4.8 Hz, 3H), 2.88–2.95 (m, 1H), 3.07 (dd, J = 13.2, 4.2 Hz, 1H), 4.56 (s, 1H), 7.28–7.57 (m, 3H), 7.74–8.23 (m, 1H), 8.39 (d, J = 5.2 Hz, 1H); ^{13}C NMR (75 MHz, DMSO- d_6): δ 34.5, 40.1, 52.7, 122.5, 131.8, 132.2, 140.1, 170.0; HRMS (ESI, positive): Calcd. for $\text{C}_{10}\text{H}_{14}\text{N}_2\text{O}$ $[\text{M}+\text{H}]^+$ 179.1179; observed: 179.1180.

6.1.6. General procedure for preparation of compounds **10a–10f**

HOBt (71 mg, 0.52 mmol) and HBTU (199 mg, 0.52 mmol) was added to a stirred solution of phenylalanine derivatives **9a–9c** (0.52 mmol) in DMF (6 mL) at rt. After the mixture was cooled to 0 °C, amines **8a–8d** (0.7 mmol) and DIEA (1 mmol) were introduced, respectively. The whole reaction mixture was stirred at rt for 12 h, the solvents and volatiles were removed under the reduced pressure. The solid residue was crystallized from dichloromethane to give the desired products as white solid.

6.1.6.1. (9*H*-Fluoren-9-yl)methyl ((*S*)-1-(((*S*)-3-(3,5-dibromophenyl)-1-(methylamino)-1-oxopropan-2-yl)amino)-3-(4-carbamoylphenyl)-1-oxopropan-2-yl)carbamate (**10a**). 76% yield; ^1H NMR (300 MHz, DMSO- d_6): δ 2.57 (d, J = 4.5 Hz, 3H), 2.73–2.85 (m, 2H), 2.94–3.01 (m, 2H), 3.40–4.47 (m, 5H), 7.19–7.43 (m, 11H), 7.58 (t, J = 3.6 Hz, 2H), 7.77–7.92 (m, 2H), 8.21 (d, J = 8.4 Hz, 1H); ^{13}C NMR (75 MHz, DMSO- d_6): δ 26.0, 37.7, 47.0, 54.2, 56.3, 66.1, 113.4, 113.7, 116.5, 120.6, 125.7, 127.8, 128.1, 129.5, 130.4, 132.7, 140.9, 141.0, 141.1, 142.0, 144.2, 156.1, 168.2, 171.3, 171.6; HRMS (ESI, positive): Calcd. for $\text{C}_{35}\text{H}_{32}\text{Br}_2\text{N}_4\text{O}_5\text{Na}$ $[\text{M}+\text{Na}]^+$ 769.0632, 771.0611; observed: 769.0630, 771.0603.

6.1.6.2. (9*H*-Fluoren-9-yl)methyl ((*S*)-1-(((*S*)-3-(3-bromophenyl)-1-(methylamino)-1-oxopropan-2-yl)amino)-3-(3-carbamoylphenyl)-1-oxopropan-2-yl)carbamate (**10b**). Fmoc-*L*-3-carbamoylphenylalanine was used for replacing Fmoc-*L*-4-carbamoylphenylalanine, as well as (*S*)-2-amino-3-(3-bromo-phenyl)-*N*-methylpropanamide replacing of (*S*)-2-amino-3-(3,5-dibromophenyl)-*N*-methylpropanamide, in the described procedure, and **10b** was obtained in 78% yield. ^1H NMR (300 MHz, DMSO- d_6): δ 2.56 (d, J = 4.5 Hz, 3H), 2.73–2.85 (m, 2H), 2.94–3.00 (m, 2H), 3.99–4.29

(m, 4H), 4.42–4.50 (m, 1H), 7.18–7.43 (m, 11H), 7.57–7.62 (m, 2H), 7.76 (d, J = 8.1 Hz, 2H), 7.86–7.91 (m, 3H), 8.20 (d, J = 8.1 Hz, 1H); ^{13}C NMR (75 MHz, DMSO- d_6): δ 25.6, 35.9, 46.6, 53.9, 54.2, 56.0, 65.8, 120.2, 121.5, 125.4, 126.4, 127.4, 127.8, 128.2, 129.3, 130.3, 132.4, 137.7, 140.6, 140.8, 141.6, 141.7, 143.8, 143.9, 155.8, 167.9, 171.0, 171.2, 171.3; HRMS (ESI, positive): Calcd. for $\text{C}_{35}\text{H}_{33}\text{BrN}_4\text{O}_5\text{Na}$ $[\text{M}+\text{Na}]^+$ 691.1527, 693.1506; observed: 691.1522, 693.1496.

6.1.6.3. (9*H*-Fluoren-9-yl)methyl ((*S*)-1-(((*S*)-3-(3-fluorophenyl)-1-(methylamino)-1-oxopropan-2-yl)amino)-3-(4-carbamoylphenyl)-1-oxopropan-2-yl)carbamate (**10c**). (*S*)-2-Amino-3-(3-fluorophenyl)-*N*-methylpropanamide was used for replacing (*S*)-2-amino-3-(3,5-dibromophenyl)-*N*-methylpropanamide in the described procedure, and **10c** was obtained in 64% yield. ^1H NMR (300 MHz, DMSO- d_6): δ 2.56 (d, J = 6.0 Hz, 3H), 2.68–2.88 (m, 2H), 2.96–3.01 (m, 2H), 4.11–4.32 (m, 4H), 4.52 (dd, J = 10.8, 6.0 Hz, 1H), 6.95–7.06 (m, 3H), 7.22–7.42 (m, 8H), 7.61 (t, J = 6.4 Hz, 3H), 7.77–7.88 (m, 8H), 7.86 (d, J = 7.5 Hz, 1H); ^{13}C NMR (75 MHz, DMSO- d_6): δ 25.7, 37.9, 38.3, 46.6, 53.9, 56.0, 65.8, 113.4, 116.2, 120.2, 125.4, 127.2, 127.8, 129.9, 130.0, 132.4, 140.7, 140.8, 141.7, 143.8, 143.9, 155.8, 160.5, 163.7, 167.9, 171.0, 171.3; HRMS (ESI, positive): Calcd. for $\text{C}_{35}\text{H}_{33}\text{FN}_4\text{O}_5\text{Na}$ $[\text{M}+\text{Na}]^+$ 631.2327; observed: 631.2322.

6.1.6.4. (9*H*-Fluoren-9-yl)methyl ((*S*)-3-(4-carbamoylphenyl)-1-(((*S*)-1-(methylamino)-1-oxo-3-phenylpropan-2-yl)amino)-1-oxopropan-2-yl)carbamate (**10d**). (*S*)-2-Amino-3-phenyl-*N*-methylpropanamide was used for replacing (*S*)-2-amino-3-(3,5-dibromophenyl)-*N*-methylpropanamide in the described procedure, and **10d** was obtained in 93% yield. ^1H NMR (300 MHz, DMSO- d_6): δ 2.56 (d, J = 6.0 Hz, 3H), 2.73–2.84 (m, 2H), 2.94 (dd, J = 10.8, 7.2 Hz, 2H), 4.12–4.29 (m, 4H), 4.52 (dd, J = 10.8, 6.2 Hz, 1H), 7.18–7.43 (m, 12H), 7.57 (t, J = 9.2 Hz, 3H), 7.76 (6, J = 10.8 Hz, 2H), 7.86–8.22 (m, 5H); ^{13}C NMR (75 MHz, DMSO- d_6): δ 25.6, 37.3, 37.6, 46.6, 53.8, 55.9, 65.7, 120.1, 125.4, 126.4, 127.1, 127.7, 128.0, 129.1, 129.9, 132.7, 140.3, 140.7, 141.6, 143.7, 143.8, 155.7, 167.8, 170.9, 171.2; HRMS (ESI, positive): Calcd. for $\text{C}_{35}\text{H}_{34}\text{N}_4\text{O}_5\text{Na}$ $[\text{M}+\text{Na}]^+$ 613.2421; observed: 631.2322.

6.1.6.5. (9*H*-Fluoren-9-yl)methyl ((*S*)-1-(((*S*)-3-(3-bromophenyl)-1-(methylamino)-1-oxopropan-2-yl)amino)-1-oxo-3-phenylpropan-2-yl)carbamate (**10e**). Fmoc-*L*-phenylalanine was used for replacing Fmoc-*L*-4-carbamoylphenylalanine, as well as (*S*)-2-amino-3-(3-bromophenyl)-*N*-methylpropanamide replacing of (*S*)-2-amino-3-(3,5-dibromophenyl)-*N*-methylpropanamide, in the described procedure, and **10e** was obtained in 67% yield. ^1H NMR (400 MHz, DMSO- d_6): δ 2.56 (d, J = 5.6 Hz, 3H), 2.68–2.88 (m, 2H), 2.95 (dd, J = 11.6, 6.8 Hz, 2H), 4.01–4.51 (m, 5H), 7.16–7.42 (m, 10H), 7.57 (t, J = 10.0 Hz, 3H), 7.78–8.25 (m, 7H); ^{13}C NMR (100 MHz, DMSO- d_6): δ 25.6, 37.7, 46.6, 53.9, 56.0, 65.8, 120.2, 125.3, 125.4, 126.5, 127.2, 127.4, 127.7, 128.1, 129.1, 130.0, 132.4, 132.8, 140.3, 140.8, 141.6, 143.8, 143.9, 167.9, 171.0, 171.3; HRMS (ESI, positive): Calcd. for $\text{C}_{34}\text{H}_{32}\text{BrN}_3\text{O}_5\text{Na}$ $[\text{M}+\text{Na}]^+$ 648.1468, 650.1448; observed: 648.1463, 650.1450.

6.1.6.6. (9*H*-Fluoren-9-yl)methyl ((*S*)-1-(((*S*)-3-(3-bromophenyl)-1-(methylamino)-1-oxopropan-2-yl)amino)-3-(4-carbamoylphenyl)-1-oxopropan-2-yl)carbamate (**10f**). (*S*)-2-Amino-3-(3-bromophenyl)-*N*-methylpropanamide was used for replacing (*S*)-2-amino-3-(3,5-dibromophenyl)-*N*-methylpropanamide in the described procedure, and **10f** was obtained in 78% yield. ^1H NMR (300 MHz, DMSO- d_6): δ 2.56 (d, J = 6.0 Hz, 3H), 2.73–2.84 (m, 2H), 2.94 (dd, J = 10.8, 7.2 Hz, 2H), 3.99–4.50 (m, 5H), 7.18–7.43 (m, 10H), 7.58 (t, J = 4.8 Hz, 2H), 7.76–8.22 (m, 6H); ^{13}C NMR (75 MHz, DMSO-

d_6): δ 25.6, 37.8, 46.6, 53.9, 54.2, 56.0, 65.8, 120.2, 121.5, 125.4, 126.4, 127.2, 127.4, 127.8, 128.2, 128.5, 129.3, 130.3, 137.7, 140.8, 141.6, 143.8, 143.9; HRMS (ESI, positive): Calcd. for $C_{34}H_{32}BrN_3O_5Na$ $[M+Na]^+$ 691.1527, 693.1506; observed: 691.1506, 693.1493.

6.1.7. General procedure for preparation of compounds **11a–11f**

Piperidine (2 mL) was added to a stirred solution of **10a–10f** (0.4 mmol) dissolved in DMF (4 mL), and the mixture was stirred at rt for 2 h. After the completion of the reaction, the solvent and volatiles were removed under reduced pressure, and the solid residue was crystallized from EtOAc to give the desired product as light brown solid.

6.1.7.1. 4-((S)-2-Amino-3-(((S)-3-(3,5-dibromophenyl)-1-(methylamino)-1-oxopropan-2-yl)amino)-3-oxopropyl)benzamide (**11a**). 76% yield; 1H NMR (300 MHz, DMSO- d_6): δ 2.57 (d, $J = 4.2$ Hz, 3H), 2.78–2.84 (m, 2H), 2.99 (dd, $J = 13.2, 4.2$ Hz, 3H), 4.46 (s, 1H), 7.18 (d, $J = 8.1$ Hz, 2H), 7.30–7.97 (m, 6H), 8.12 (d, $J = 3.9$ Hz, 1H), 8.29–8.30 (m, 2H); ^{13}C NMR (75 MHz, DMSO- d_6): δ 25.7, 37.2, 40.1, 53.2, 56.3, 122.1, 127.5, 129.1, 131.4, 131.5, 132.2, 142.2, 143.0, 167.9, 170.8, 174.0; HRMS (ESI, positive): Calcd. for $C_{20}H_{22}Br_2N_4O_3Na$ $[M+Na]^+$ 546.9951, 548.9930; observed: 546.9947, 548.9930.

6.1.7.2. 3-((S)-2-Amino-3-(((S)-3-(3-bromophenyl)-1-(methylamino)-1-oxopropan-2-yl)amino)-3-oxopropyl)benzamide (**11b**). 75% yield; 1H NMR (300 MHz, DMSO- d_6): δ 2.59 (d, $J = 6.0$ Hz, 3H), 2.73–2.81 (m, 1H), 2.95 (dd, $J = 13.8, 4.2$ Hz, 1H), 4.09–4.19 (m, 4H), 7.23–7.43 (m, 7H), 7.54 (s, 1H), 7.64 (t, $J = 6.6$ Hz, 2H), 7.70 (d, $J = 8.7$ Hz, 1H), 7.87–8.01 (m, 3H); ^{13}C NMR (75 MHz, DMSO- d_6): δ 26.0, 38.0, 44.6, 53.6, 56.6, 121.8, 126.9, 127.8, 128.8, 129.5, 129.7, 130.7, 132.5, 132.6, 141.1, 142.3, 142.6, 168.2, 171.4, 174.3; HRMS (ESI, positive): Calcd. for $C_{20}H_{23}BrN_4O_3Na$ $[M+Na]^+$ 469.084, 471.0825; observed: 469.0841, 471.0825.

6.1.7.3. 4-((S)-2-Amino-3-(((S)-3-(3-fluorophenyl)-1-(methylamino)-1-oxopropan-2-yl)amino)-3-oxopropyl)benzamide (**11c**). 79% yield; 1H NMR (300 MHz, DMSO- d_6): δ 2.57 (d, $J = 3.6$ Hz, 3H), 2.72–2.95 (m, 4H), 3.38 (d, $J = 4.2$ Hz, 1H), 6.97 (d, $J = 10.4$ Hz, 2H), 7.18–7.31 (m, 3H), 7.75 (d, $J = 7.8$ Hz, 2H), 7.93–8.16 (m, 3H); ^{13}C NMR (75 MHz, DMSO- d_6): δ 25.6, 37.6, 43.8, 53.3, 56.7, 121.4, 127.4, 128.4, 129.1, 129.3, 130.3, 132.1, 132.2, 140.7, 142.1, 167.8, 170.9, 173.8; HRMS (ESI, positive): Calcd. for $C_{20}H_{23}FN_4O_3Na$ $[M+Na]^+$ 409.1646; observed: 409.1646.

6.1.7.4. 4-((S)-2-Amino-3-(((S)-1-(methylamino)-1-oxo-3-phenylpropan-2-yl)amino)-3-oxopropyl)benzamide (**11d**). 90% yield; 1H NMR (300 MHz, DMSO- d_6): δ 2.56 (d, $J = 4.8$ Hz, 3H), 2.76–2.98 (m, 4H), 3.16 (s, 1H), 4.45 (d, $J = 5.1$ Hz, 1H), 7.14–7.39 (m, 7H), 7.75 (d, $J = 8.4$ Hz, 2H), 7.90–8.13 (m, 3H); ^{13}C NMR (75 MHz, DMSO- d_6): δ 25.7, 37.7, 40.1, 53.3, 56.2, 121.5, 127.5, 128.5, 129.4, 130.4, 132.3, 140.7, 142.3, 167.9, 171.0, 174.0; HRMS (ESI, positive): Calcd. for $C_{20}H_{24}N_4O_3Na$ $[M+Na]^+$ 391.1741; observed: 391.1741.

6.1.7.5. (S)-2-Amino-N-((S)-3-(3-bromophenyl)-1-(methylamino)-1-oxopropan-2-yl)-3-phenylpropanamide (**11e**). 90% yield; 1H NMR (400 MHz, DMSO- d_6): δ 2.59 (d, $J = 6.0$ Hz, 3H), 2.73–2.81 (m, 1H), 2.96 (dd, $J = 14.8, 5.6$ Hz, 1H), 4.09–4.20 (m, 4H), 7.19–7.33 (m, 5H), 7.38–7.45 (m, 4H), 7.53 (s, 1H), 7.61–7.71 (m, 3H), 7.86 (d, $J = 10.0$ Hz, 2H), 7.99 (d, $J = 6.0$ Hz, 1H); ^{13}C NMR (100 MHz, DMSO- d_6): δ 5.7, 37.7, 40.4, 53.3, 56.2, 121.5, 127.5, 128.5, 129.2, 129.4, 130.4, 132.1, 132.3, 140.7, 142.3, 167.9, 174.0; HRMS (ESI, positive): Calcd. for $C_{19}H_{22}BrN_3O_2Na$ $[M+Na]^+$ 426.0788, 428.0764; observed: 426.0783, 428.0764.

6.1.7.6. 4-((S)-2-Amino-3-(((S)-3-(3-bromophenyl)-1-(methylamino)-1-oxopropan-2-yl)amino)-3-oxopropyl)benzamide (**11f**). 95% yield; 1H NMR (300 MHz, DMSO- d_6): δ 2.60 (d, $J = 4.5$ Hz, 3H), 2.77–2.85 (m, 1H), 2.97 (dd, $J = 13.5, 4.2$ Hz, 1H), 4.09–4.22 (m, 4H), 6.99–7.17 (m, 3H), 7.25–7.43 (m, 5H), 7.61–7.89 (m, 6H); ^{13}C NMR (75 MHz, DMSO- d_6): δ 25.7, 37.7, 44.1, 53.4, 56.3, 126.5, 127.5, 128.2, 129.2, 129.3, 130.0, 132.2, 132.7, 140.5, 142.3, 167.9, 171.1, 174.1; HRMS (ESI, positive): Calcd. for $C_{20}H_{23}BrN_4O_3Na$ $[M+Na]^+$ 469.0846, 471.0825; observed: 469.0845, 471.0827.

6.1.8. Procedure for preparation of 2-cyclohexyl-2-(4-methoxyphenyl)acetic acid (**14b**, $R_4 = OMe$) and 2-cyclohexyl-2-(4-hydroxyphenyl)acetic acid (**14c**, $R_4 = OH$)

To a stirred solution of cyclohexanol (5g, 50 mmol) in pyridine (180 mL) was added 4-methylbenzenesulfonyl chloride (14.3 g, 75 mmol) at 0 °C. The reaction mixture was stirred at rt for 12 h or until the material completely disappeared as checked by TLC. After removal of solvent by a rotary evaporator, the crude product was purified by flash column chromatograph (eluting with hexane: EtOAc, 50:1) to afford 4-methylbenzenesulfonate (**13**) (10.1 g, 79% yield) as whit solid. 1H NMR (300 MHz, $CDCl_3$): δ 1.24–1.31 (m, 3H), 1.45–1.57 (m, 3H), 1.66–1.80 (m, 4H), 2.44 (s, 3H), 4.45 (m, 1H), 7.32–7.34 (m, 2H), 7.78–7.81 (m, 2H); ^{13}C NMR (75 MHz, $CDCl_3$): δ 21.7, 23.5, 24.9, 32.4, 81.8, 127.6, 129.8, 134.8, 144.4; HRMS (ESI, negative): Calcd. for $C_{13}H_{18}O_3S[M-1]^-$ 253.0904; observed: 253.0901.

To a stirred solution of 2-(4-methoxyphenyl)acetic acid (2.5 g, 15 mmol) in THF (125 mL) was added slowly *n*-BuLi (18 mL, 2.5 M hexane solution, 45 mmol) at –78 °C. 30 min later, **13** (3.8 g, 15 mmol) was added, and the mixture was stirred for an additional 1 h at –78 °C, and then allowed to warm to ambient temperature with the stirring was continued for 12 h. The reaction was quenched by adding H_2O (10 mL). After removal of solvents by a rotary evaporator, the crude product was purified by flash column chromatograph (eluting with DCM:MeOH, 100:1) to afford **14b** (1.7 g, 43% yield) as white solid. M.p. 177–178 °C; 1H NMR (300 MHz, $CDCl_3$): δ 0.68–0.77 (m, 4H), 1.02–1.36 (m, 2H), 1.61–2.05 (m, 5H), 3.15 (d, $J = 10.5$ Hz, 1H), 3.78 (s, 3H), 6.82 (dd, $J = 6.6, 1.3$ Hz, 2H), 7.22 (dd, $J = 6.9, 2.1$ Hz, 2H); ^{13}C NMR (75 MHz, $CDCl_3$): δ 26.1, 26.4, 30.4, 32.1, 40.8, 55.4, 58.1, 114.0, 129.4, 129.8, 159.0, 180.7; HRMS (ESI, negative): Calcd. for $C_{15}H_{20}O_3[M-1]^-$ 247.1340; observed: 247.1343.

BBr_3 (5.4 mL, 58 mmol) was added dropwise to an ice-cold stirred solution of **14b** (1.2 g, 4.8 mmol) in DCM (20 mL). The mixture was stirred at 0 °C for 4 h, and then allowed to warm to ambient temperature with the stirring continued for additional 36 h. The reaction was quenched by adding H_2O (30 mL), and the resulting mixture was extracted with DCM (3 \times 120 mL). The combined extracts were washed with brine (2 \times 80 mL), and dried. The crude product was purified by flash column chromatograph (DCM:MeOH, 40:1) to afford **14c** (600 mg, 55% yield) as white solid. 1H NMR (300 MHz, $CDCl_3$): δ 1.06–1.23 (m, 4H), 1.27–1.35 (m, 2H), 1.61–1.95 (m, 5H), 3.06 (d, $J = 8.1$ Hz, 1H), 6.71 (d, $J = 6.6$ Hz, 2H), 7.12 (d, $J = 6.6$ Hz, 2H); ^{13}C NMR (75 MHz, $CDCl_3$): δ 27.1, 27.5, 31.4, 33.1, 42.0, 59.4, 116.1, 130.3, 130.5, 157.6, 178.2; HRMS (ESI, negative): Calcd. for $C_{14}H_{18}O_3[M-1]^-$ 233.1183; observed: 233.1187.

6.1.9. General procedure for preparation of the title compounds (**15A1–15A7**)

HOBt (75 mg, 0.56 mmol) and HBTU (211 mg, 0.56 mmol) were added to a stirred solution of substituted 2-phenylacetic acid **14a–14c** (0.56 mmol) in DMF (5 mL) at rt. After the mixture was cooled to 0 °C, dipeptide amine **11a–11e** (0.28 mmol) was added, respectively, followed by addition of DIEA (0.84 mmol). The reaction mixture was stirred at ambient temperature for 12 h, and the solvent and volatiles were evaporated under the reduced pressure, and

then the solid residue was crystallized from EtOAc to generate the desired product as white solid.

6.1.9.1. (2*S*)-3-(3-Bromophenyl)-2-((2*S*)-2-(2-cyclohexyl-2-phenylacetamido)-3-phenylpropan-amido)-*N*-methylpropanamide (**15A1**). 70% yield; ¹H NMR (300 MHz, DMSO-*d*₆): δ 0.61–0.90 (m, 2H), 1.08–1.56 (m, 7H), 2.21–2.47 (m, 2H), 2.55 (d, *J* = 3.3 Hz, 3H), 2.66–3.02 (m, 4H), 3.22 (d, *J* = 8.1 Hz, 1H), 6.98–7.04 (m, 2H), 7.13–7.43 (m, 9H), 7.55 (d, *J* = 6.0 Hz, 1H), 7.77–7.90 (m, 3H), 8.15 (t, *J* = 7.8 Hz, 2H); ¹³C NMR (75 MHz, DMSO-*d*₆): δ 25.6, 26.2, 30.3, 31.3, 37.6, 53.4, 53.5, 53.8, 53.9, 58.0, 110.3, 118.9, 121.5, 123.9, 126.4, 127.2, 128.0, 128.3, 128.5, 129.4, 130.2, 131.9, 139.4, 140.6, 167.8, 171.0, 172.5; HRMS (ESI, positive): Calcd. for C₃₃H₃₈BrN₃O₃Na [M+Na]⁺ 626.1989, 628.1968; observed: 626.1985, 628.1971.

6.1.9.2. 3-((2*S*)-3-(((*S*)-3-(3-Bromophenyl)-1-(methylamino)-1-oxopropan-2-yl)amino)-2-(2-cyclohexyl-2-phenylacetamido)-3-oxopropyl)benzamide (**15A2**). 81% yield; ¹H NMR (300 MHz, DMSO-*d*₆): δ 0.41–0.64 (m, 2H), 0.79–1.23 (m, 5H), 1.34–1.59 (m, 3H), 1.88 (d, *J* = 13.6 Hz, 1H), 2.55 (d, *J* = 6.0 Hz, 3H), 2.63–3.05 (m, 4H), 3.16 (d, *J* = 14.4 Hz, 1H), 4.26–4.64 (m, 2H), 6.95 (t, *J* = 10.0 Hz, 3H), 7.15–7.33 (m, 9H), 7.38–7.41 (m, 1H), 7.51 (d, *J* = 10.8 Hz, 1H), 7.77–7.79 (m, 2H), 8.09–8.22 (m, 2H); ¹³C NMR (75 MHz, DMSO-*d*₆): δ 25.9, 26.0, 26.5, 30.7, 31.6, 37.6, 37.9, 53.9, 54.2, 58.3, 121.8, 126.8, 127.7, 128.7, 128.8, 139.6, 130.6, 132.3, 132.4, 132.5, 139.8, 140.0, 140.7, 140.9, 141.2, 141.8, 168.0, 168.1, 171.1, 172.8; HRMS (ESI, positive): Calcd. For C₃₄H₃₉BrN₄O₄Na [M+Na]⁺ 669.2047, 671.2026; observed: 669.2047, 671.2034.

6.1.9.3. 4-((2*S*)-2-(2-Cyclohexyl-2-phenylacetamido)-3-(((*S*)-1-(methylamino)-1-oxo-3-phenylpropan-2-yl)amino)-3-oxopropyl)benzamide (**15A3**). 81% yield; ¹H NMR (300 MHz, DMSO-*d*₆): δ 0.84–1.07 (m, 2H), 1.10–1.20 (m, 3H), 1.55–1.90 (m, 6H), 2.50 (d, *J* = 0.9 Hz, 3H), 2.52–2.99 (m, 4H), 3.17 (d, *J* = 10.8 Hz, 1H), 4.41–4.44 (m, 2H), 6.96–7.43 (m, 14H), 7.35 (d, *J* = 8.1 Hz, 1H), 7.78–8.17 (m, 4H); ¹³C NMR (75 MHz, DMSO-*d*₆): δ 25.7, 26.0, 26.5, 30.7, 31.6, 37.6, 37.9, 53.9, 54.2, 58.3, 121.8, 126.8, 127.7, 128.6, 128.8, 129.7, 130.7, 132.3, 132.5, 140.0, 140.9, 141.8, 168.0, 168.1, 171.3, 172.8; HRMS (ESI, positive): Calcd. for C₃₄H₄₀N₄O₄Na [M+Na]⁺ 591.2942; observed: 591.2937.

6.1.9.4. 4-((2*S*)-3-(((*S*)-3-(3-Fluorophenyl)-1-(methylamino)-1-oxopropan-2-yl)amino)-2-(2-cyclohexyl-2-phenylacetamido)-3-oxopropyl)benzamide (**15A4**). 41% yield; ¹H NMR (300 MHz, DMSO-*d*₆): δ 0.41–0.64 (m, 2H), 0.85–1.23 (m, 4H), 1.34–1.58 (m, 4H), 1.72–1.90 (m, 1H), 2.54 (d, *J* = 4.2 Hz, 3H), 2.68–3.05 (m, 4H), 3.23 (d, *J* = 1.8 Hz, 1H), 4.30–4.64 (m, 2H), 6.86–7.33 (m, 14H), 7.52 (d, *J* = 8.1 Hz, 1H), 7.77–8.28 (m, 3H); ¹³C NMR (75 MHz, DMSO-*d*₆): δ 24.9, 25.2, 30.6, 30.8, 31.1, 37.6, 37.9, 43.3, 53.9, 37.4, 121.8, 126.8, 127.7, 128.4, 128.6, 129.3, 129.7, 130.6, 132.3, 132.6, 140.8, 141.0, 141.3, 141.7, 168.1, 171.0, 171.2, 173.1; HRMS (ESI, positive): Calcd. for C₃₄H₃₉FN₄O₄Na [M+Na]⁺ 609.2848; observed: 609.2845.

6.1.9.5. 4-((2*S*)-3-(((*S*)-3-(3,5-Dibromophenyl)-1-(methylamino)-1-oxopropan-2-yl)amino)-2-(2-cyclohexyl-2-phenylacetamido)-3-oxopropyl)benzamide (**15A5**). 50% yield; ¹H NMR (300 MHz, DMSO-*d*₆): δ 0.46–0.65 (m, 1H), 0.83–1.20 (m, 5H), 1.43–1.91 (m, 5H), 2.49 (d, *J* = 4.5 Hz, 3H), 2.59–2.95 (m, 3H), 3.02 (d, *J* = 10.8 Hz, 2H), 4.22–4.60 (m, 2H), 6.87–7.27 (m, 14H), 7.64–7.73 (m, 1H), 7.97–8.21 (m, 2H); ¹³C NMR (75 MHz, DMSO-*d*₆): δ 25.6, 25.7, 26.2, 30.3, 31.3, 37.2, 37.4, 53.8, 54.0, 58.0, 122.2, 126.5, 127.4, 128.6, 129.3, 131.5, 132.0, 139.6, 141.0, 141.5, 142.7, 142.9, 167.9, 170.8, 171.2, 172.5; HRMS (ESI, positive): Calcd for C₃₄H₃₈Br₂N₄O₄Na [M+Na]⁺ 747.1152, 749.1132; observed: 747.1151, 749.1138.

6.1.9.6. 4-((2*S*)-3-(((*S*)-3-(3-Bromophenyl)-1-(methylamino)-1-oxopropan-2-yl)amino)-2-(2-cyclohexyl-2-(4-hydroxyphenyl)acetamido)-3-oxopropyl)benzamide (**15A6**). 74% yield; ¹H NMR (300 MHz, DMSO-*d*₆): δ 0.40–0.63 (m, 2H), 0.79–1.23 (m, 4H), 1.35–1.56 (m, 4H), 1.75–1.83 (m, 1H), 2.55 (d, *J* = 4.2 Hz, 3H), 2.67–3.10 (m, 5H), 4.31–4.63 (m, 2H), 6.63 (d, *J* = 6.2 Hz, 2H), 7.00–7.43 (m, 11H), 7.58–7.92 (m, 4H), 8.04–8.18 (m, 2H), 9.25 (s, 1H); ¹³C NMR (75 MHz, DMSO-*d*₆): δ 26.0, 26.6, 30.7, 31.7, 37.5, 37.9, 53.9, 54.0, 54.3, 57.5, 115.2, 119.0, 121.9, 127.7, 128.7, 129.5, 130.0, 130.7, 132.3, 132.5, 140.8, 141.0, 141.8, 156.4, 168.2, 171.1, 171.4, 173.4; HRMS (ESI, positive): Calcd for C₃₄H₃₉BrN₄O₅Na [M+Na]⁺ 685.1996, 687.1976; observed: 685.2000, 687.1989.

6.1.9.7. 4-((2*S*)-3-(((*S*)-3-(3-Bromophenyl)-1-(methylamino)-1-oxopropan-2-yl)amino)-2-(2-cyclohexyl-2-(4-methoxyphenyl)acetamido)-3-oxopropyl)benzamide (**15A7**). 70% yield; ¹H NMR (300 MHz, DMSO-*d*₆): δ 0.40–0.63 (m, 2H), 0.85–0.95 (m, 2H), 1.07–1.23 (m, 3H), 1.34–1.87 (m, 4H), 2.55 (d, *J* = 3.6 Hz, 3H), 2.64–3.01 (m, 4H), 3.09 (d, *J* = 8.1 Hz, 1H), 3.68 (d, *J* = 10 Hz, 3H), 4.27–4.65 (m, 2H), 6.75–6.81 (m, 2H), 7.00–7.08 (m, 5H), 7.15–7.41 (m, 5H), 7.54 (d, *J* = 6.0 Hz, 1H), 7.77–8.15 (m, 4H); ¹³C NMR (75 MHz, DMSO-*d*₆): δ 26.0, 26.5, 30.6, 31.0, 31.6, 37.6, 37.9, 53.9, 54.2, 55.4, 57.4, 113.7, 121.8, 127.7, 128.7, 129.3, 129.5, 129.7, 130.7, 131.9, 132.4, 140.8, 141.3, 141.8, 158.3, 168.1, 171.1, 172.9, 173.2; HRMS (ESI, positive): Calcd for C₃₅H₄₁BrN₄O₅Na [M+Na]⁺ 699.2153, 701.2132; observed: 699.2149, 701.2144.

6.2. Cell-based activity assays

6.2.1. Measurements of cAMP production

Glosensor (Promega) was used to monitor the level of cAMP as described previously¹⁴ with slight modifications. HEK-293 cells expressing a chemiluminescence-based cAMP biosensor were plated in 96-well plates at a density of 80,000 cells per well. On the following day, the cells were incubated in an incubator at 27 °C for 1 h after adding the Glosensor reagent. Subsequently, cells were treated with either 0.5% DMSO or Cmpd-15 derivatives at different concentrations in HANK's balanced solution (Sigma), which also contained 20 mM HEPES, pH 7.4, 0.05% bovine serum albumin (BSA) and 3-isobutyl-1-methylxanthine (IBMX; Sigma) at 100 μM as the final concentration. The cells were further incubated for 20 min, and then stimulated with a serial dilution of ISO for 5 min at ambient temperature. A NOVOstar microplate reader (BMG Labtech) was used to read the luminescence signals.

6.2.2. Measurements of β-arrestin recruitment

PathHunter, an enzyme fragment complementation assay (DiscoverRx)¹⁵ was used to monitor the extent of β-arrestin recruitment as described previously¹⁴ with slight modifications. U2OS cells, stably expressing enzyme acceptor-tagged β-arrestin2 and the ProLink-tagged β₂V₂R were plated in 96-well plates at a density of 25,000 cells per well. Similar to the Glosensor assay, the cells were pre-treated with 0.5% DMSO or Cmpd-15 derivatives. Subsequently, cells were stimulated with agonists at 37 °C for 45 min, and were then terminated by adding the PathHunter detection reagents (DiscoverRx). After further incubation at 27 °C for an additional hour, a NOVOstar microplate reader (BMG Labtech) was used to read the luminescence signals.

6.3. Radioligand binding assays

The reaction mixture (250 μL) was composed of ~0.7 ng the β₂AR in nanodiscs, 60 pM [¹²⁵I]-cyanopindolol (CYP) (2200 Ci/mmol; PerkinElmer), Cmpd-15 derivatives and ISO (at different concentrations). Nonspecific binding was determined using 20 μM propranolol. Every component in the mixture was diluted in

the binding buffer (20 mM Hepes, pH 7.4, 100 mM NaCl) supplemented with 0.1% BSA, and 1 mM ascorbic acid. After a 90-min incubation at ambient temperature, the binding assays were filtered onto GF/B glass-fiber filters (Brandel), which was pre-treated with 0.3% polyethyleneimine, followed by washing with 8 mL of the binding buffer using a harvester (Brandel). A Packard Cobra Quantum gamma counter (Packard) was used to quantify the bound [¹²⁵I].

6.4. Data analysis

All dose-response curve fits were performed using the computer program GraphPad Prism. Statistical analysis for percentage decreases relative to Cmpd-15 blockade levels in Table 1 and fold shifts of the EC₅₀ values in Table 2 were conducted using a one-way ANOVA with Dunnett's multiple comparison tests. *P < 0.05; **P < 0.01; ***P < 0.001, compared with the value of Cmpd-15.

Acknowledgments

We are grateful to the generous support and encouragement from Professor Robert J. Lefkowitz of Duke University Medical Center, USA. This work was financially supported by the National Science Foundation of China (grant 21292029) and Changzhou Science & Technology Program, China (CJ20160056).

A. Supplementary data

¹H NMR and ¹³C NMR spectra of the compounds described in Experimental Section. Supplementary data associated with this article can be found, in the online version, at <https://doi.org/10.1016/j.bmc.2018.03.023>.

References

1. Lefkowitz RJ. Seven transmembrane receptors: something old, something new. *Acta Physiol (Oxf)*. 2007;190:9–19.
2. Hall RA, Premont RT, Chow CW, et al. The β₂-adrenergic receptor interacts with the Na⁺/H⁺-exchanger regulatory factor to control Na⁺/H⁺ exchange. *Nature*. 1998;392:626–630.
3. Cruickshank JM. Beta blockers in hypertension. *Lancet*. 2010;376:415.
4. Tomiyama H, Yamashina A. Beta-blockers in the management of hypertension and/or chronic kidney disease. *Int J Hypertens*. 2014;2014:919256.
5. Thanawala VJ, Forkuo GS, Stallaert W, Leff P, Bouvier M, Bond R. Ligand bias prevents class equality among beta-blockers. *Curr Opin Pharmacol*. 2014;16:50–57.
6. Weberpals J, Jansen L, Carr PR, Hoffmeister M, Brenner H. Beta blockers and cancer prognosis- The role of immortal time bias: A systematic review and meta-analysis. *Cancer Treat Rev*. 2016;47:1–11.
7. Ahn S, Kahsai AW, Pani B, et al. Allosteric "beta-blocker" isolated from a DNA-encoded small molecule library. *Proc Natl Acad Sci USA*. 2017;114:1708–1713.
8. Liu X, Ahn S, Kahsai AW, et al. Mechanism of intracellular allosteric β₂AR antagonist revealed by X-ray crystal structure. *Nature*. 2017;548:480–484.
9. Corey EJ, Feng X, Noe MC. A rational approach to catalytic enantioselective enolate alkylation using a structurally rigidified and defined chiral quaternary ammonium salt under phase transfer conditions. *J Am Chem Soc*. 1997;119:12414–12415.
10. Nun P, Perez V, Calmes M, Martinez J, Lamaty F. Preparation of chiral amino esters by asymmetric phase-transfer catalyzed alkylations of Schiff bases in a ball mill. *Chem Eur J*. 2012;18:3773–3779.
11. Wu YC, Bernadat G, Masson G, Couturier C, Schlama T, Zhu J. Synthetic studies on (-)-Lemonomycin: an efficient asymmetric synthesis of lemonomycinamide. *J Org Chem*. 2009;74:2046–2052.
12. Wang Q, Zhao S, Jin L, Chen X. Synthesis of Fmoc-protected (S)-3,5-dibromophenylalanine in the presence of a phase transfer catalyst or a chiral catalyst. *Chin J Org Chem*. 2016;36:2242–2246.
13. Wang XJ, Xu B, Mullins AB, Neiler FK, Etkorn FA. Conformationally locked isostere of phosphoSer-cis-Pro inhibits Pin1 23-fold better than phosphoSer-trans-Pro isostere. *J Am Chem Soc*. 2004;126:15533–15542.
14. Rajagopal S, Ahn S, Rominger DH, et al. Quantifying ligand bias at seven-transmembrane receptors. *Mol Pharmacol*. 2011;80:367–377.
15. Bassoni DL, Raab WJ, Achacoso PL, Loh CY, Wehrman TS. Measurements of β-arrestin recruitment to activated seven transmembrane receptors using enzyme complementation. *Methods Mol Biol*. 2012;897:181–203.